

Single-crystal X-ray diffraction studies of synthetic Ni-Mg olivine solid solutions

DAN BOSTRÖM

Department of Inorganic Chemistry, University of Umeå, S-901 87 Umeå, Sweden

ABSTRACT

The structures of seven olivines of various compositions in the system $\text{Ni}_2\text{SiO}_4\text{-Mg}_2\text{SiO}_4$ have been investigated by single-crystal X-ray diffraction methods. Crystals with intermediate compositions were synthesized at 900°C. To avoid zoning, the temperature was kept constant throughout the entire preparation period. The observed cation ordering is clearly dependent on composition. The K_D values, where $K_D = [\text{Mg}_{\text{M}_2}][\text{Ni}_{\text{M}_1}]/[\text{Mg}_{\text{M}_1}][\text{Ni}_{\text{M}_2}]$, increase when the composition approaches the end members. A minimum value of $K_D \approx 10$ was obtained for $X_{\text{Ni}^{2+}} \approx 0.65$. The geometric parameters of the octahedral sites M1 and M2 are correlated more linearly with their total cation content than with the occupancy of a specific octahedron.

INTRODUCTION

The intracrystalline cation partitioning in olivines has attracted considerable attention during recent decades. In particular, the distribution of the major divalent cations in natural olivines, Fe^{2+} and Mg^{2+} , has been the subject of a number of studies [see Brown (1980) and Lumpkin and Ribbe (1983)]. Most results indicate that the distribution of Fe^{2+} and Mg^{2+} between the M1 and M2 sites is close to random.

Among the minor cation constituents in natural olivines, Ni^{2+} is common and important. Matsui and Syono (1968) examined the $(\text{Ni},\text{Mg})_2\text{SiO}_4$ solid solution using X-ray powder diffraction to determine the variation in the unit-cell dimensions with composition. They reported an excess volume of mixing and concluded that the solid solution behavior was complex. Through a single-crystal X-ray study of a synthetic olivine, $(\text{Ni}_{0.52}\text{Mg}_{0.48})_2\text{SiO}_4$, Rajamani et al. (1975) obtained a K_D value of 9.22, where $K_D = [\text{Mg}_{\text{M}_2}][\text{Ni}_{\text{M}_1}]/[\text{Mg}_{\text{M}_1}][\text{Ni}_{\text{M}_2}]$, thus indicating a strong preference of Ni^{2+} for the M1 site. Bish (1981) confirmed the strong tendency for cation ordering; one natural ($X_{\text{Ni}^{2+}} = 0.76$) and one synthetic ($X_{\text{Ni}^{2+}} = 0.58$) crystal were studied. The former was fully ordered ($K_D = \infty$), and the latter had a K_D value of 9.9.

All these results indicate a strong preference of Ni^{2+} for the M1 site, but do not allow the equilibrium distribution of Ni^{2+} and Mg^{2+} between the M1 and M2 sites, with respect to temperature and composition, to be extracted. The aim of the present study is to evaluate the behavior of the (Ni,Mg) olivine solid solution as a function of composition at a defined equilibration temperature. For this purpose, the end-member phases Ni_2SiO_4 and Mg_2SiO_4 and crystals with five intermediate compositions (see Table 1) were investigated by single-crystal X-ray diffraction techniques.

EXPERIMENTAL DETAILS

Preparation of single crystals

The crystals were grown by a flux method, using Li_2MoO_4 as the solvent. Mixtures of the starting materials Li_2CO_3 , SiO_2 , NiO , and MgO were placed in a Pt crucible and heated to 900°C in a tube furnace (see Table 1 for further synthesis conditions). Difficulties in achieving sufficiently large crystals of the end-member phases Ni_2SiO_4 and Mg_2SiO_4 at 900°C resulted in the use of 1000°C for these cases. The temperature was kept constant to within $\pm 2^\circ\text{C}$. The Pt crucibles were not completely sealed, and a small amount of the flux was evaporated to increase the olivine/flux ratio. Crystal growth was interrupted by removal of the crucibles from the furnace, followed by immediate quenching in ice.

Microprobe analysis of the crystals yielded the compositions ($X_{\text{Ni}^{2+}}$) given in Table 1. No zoning or other inhomogeneities were detected in the crystals. For details of the analytical procedure, see Princivalle and Secco (1985).

X-ray data collection

The dimensions of the orthorhombic unit cell were determined by least-squares refinement of 20 to 24 automatically centered $K\alpha_1$ reflections with $\sin \theta/\lambda \approx 1.1 \text{ \AA}^{-1}$, to ensure good separation of the α_1 and α_2 peaks. X-ray data were collected at room temperature using a Nicolet R3 four-circle diffractometer, with graphite-monochromatized $\text{MoK}\alpha$ radiation ($\lambda = 0.71069 \text{ \AA}$), and θ - 2θ scan mode ($4.6^\circ \leq 2\theta \leq 80^\circ$). The test reflections showed variations of $\approx 3\%$. The reflection intensities and backgrounds were obtained using the Lehmann-Larsen method (1974), except for the compositions $X_{\text{Ni}^{2+}} = 0.69$ and 0.36. Here a conventional background-peak-background measurement of intensity was applied. Lorentz polarization and absorption corrections were also made; the latter by an empirical method supplied with the Nicolet R3 crystallographic system. Additional experimental details are listed in Table 2.

TABLE 1. Crystal synthesis

Starting materials							
Li ₂ CO ₃ (g)	6.3765	6.3765	6.3765	6.3765	6.3765	6.3765	6.3765
MoO ₃ (g)	12.4216	12.4216	12.4216	12.4216	12.4216	12.4216	12.4216
NiO (g)		0.1420	0.1996	0.2617	0.5627	1.1208	2.0000
MgO (g)	0.5364	0.2297	0.2125	0.1412	0.1495	0.2015	
SiO ₂ (g)	0.4402	0.2283	0.2170	0.2105	0.3377	0.6071	0.8124
Duration (d)	4	5	6	7	5	14	10
Temperature (°C)	1000 (1)	902 (1)	901 (1)	890 (2)	900 (1)	910 (2)	1003 (1)
Composition X _{Ni²⁺}	0.00	0.30	0.36	0.51	0.69	0.75	1.00

Refinements

The refinements were carried out in space group *Pbnm* using the least-squares program UPALS (Lundgren, 1982). Scattering factors for neutral atoms with corrections for anomalous dispersion were taken from *International Tables for X-ray Crystallography* (1974, p. 99, 149). The atomic parameters given by Bish (1981) were used as the initial model for X_{Ni²⁺} = 0.51. The final parameters thus obtained then served as a starting model for the other structures. The compositions of the olivine solid solutions were constrained to the results from the microprobe analyses. When allowed to vary, however, the refined compositions agreed well with the microprobe result. A modified version of the Cruickshank weighting scheme was applied (Cruickshank, 1965). The final refinement cycles varied one overall scale factor, six anisotropic (one isotropic for X_{Ni²⁺} = 0.00, 0.36, 0.75) secondary extinction parameters, and positional and anisotropic temperature factors together with occupancy factors for M1 and M2. The fractional coordinates obtained for the various compositions are listed in Table 3. Anisotropic temperature coefficients and interatomic angles are listed in Tables 4 and 5, respectively. Observed and calculated structure factors are available in Tables 9a to 9g.¹

RESULTS AND DISCUSSION

The olivine structure has been discussed in detail by many authors; the interested reader is referred to Brown (1980) for a description of the structure.

¹ To obtain a copy of Table 9, order Document AM-87-350 from the Business Office, Mineralogical Society of America, 1625 I Street, N.W., Suite 414, Washington, D.C. 20006, U.S.A. Please remit \$5.00 in advance for the microfiche.

TABLE 2. Crystal data

	X _{Ni²⁺}						
	0.00	0.30	0.36	0.51	0.69	0.75	1.00
Cell dimensions							
<i>a</i> (Å)	4.7549 (3)	4.7447 (3)	4.7437 (4)	4.7389 (5)	4.7352 (5)	4.7331 (4)	4.7296 (3)
<i>b</i> (Å)	10.1985 (6)	10.1993 (6)	10.1947 (6)	10.1830 (8)	10.1612 (9)	10.1565 (13)	10.1209 (6)
<i>c</i> (Å)	5.9792 (4)	5.9567 (4)	5.9508 (4)	5.9430 (5)	5.9317 (6)	5.9285 (6)	5.9150 (4)
<i>V</i> (Å ³)	289.95 (3)	288.26 (3)	287.79 (3)	286.78 (4)	285.40 (5)	284.99 (5)	283.14 (3)
Number of reflections with <i>I</i> > 3σ(<i>I</i>)	874	921	903	915	912	915	858
Scan speed (deg/min)	0.5–2.0	0.5–2.0	2.0–6.0	0.5–2.0	2.0–6.0	0.5–2.0	0.5–2.0
Final value of <i>R</i> *	3.27	3.44	2.28	2.74	2.58	3.20	3.18
<i>R</i> _w **	3.89	4.29	2.71	3.48	3.28	3.39	3.80
<i>K</i> _D value		16.9	14.9	11.8	9.5	10.9	

* $R = (\sum(|F_o| - |F_c|) / \sum |F_o|) \cdot 100\%$.

** $R_w = (\sum w(|F_o| - |F_c|)^2 / \sum w F_o^2)^{1/2} \cdot 100\%$.

Cation distribution

The *K*_D values given in Table 2 and plotted in Figure 1a are calculated from the occupancy factors given in Table 3; the estimated error on the *K*_D values is <0.5. The *K*_D curve shows the magnitude of the ordering at 900°C for different compositions. The ordering has a minimum at X_{Ni²⁺} ≈ 0.65 and increases toward the end members.

Another way of displaying the cation partitioning is given in Figure 1b, where the distribution of Ni²⁺ on M1 and M2 is shown. This presentation is more useful than the *K*_D curve for discussing structural geometries.

M1 octahedron

Neither the mean bond distance M1–O nor the individual bond distances show any significant departure from linearity with respect to cation composition X_{Ni²⁺} (Table 6, Fig. 2). Two bonds in pure Mg₂SiO₄, M1–O(1) and M1–O(2), differ by 0.016 Å, but they approach each other with increasing Ni content and coincide completely in pure Ni₂SiO₄. Note that the M1–O(2) bond length is almost constant throughout the entire composition range.

As shown in Figure 3, the volume of the M1 octahedron has a slight positive deviation from linearity with respect to X_{Ni²⁺}. A negative deviation would be expected, however, considering the Ni²⁺ content of M1 (cf. Fig. 1b) and the smaller ionic radius of Ni²⁺. On the other hand, the distortion parameter octahedral-angle variance (OAV) (Fig. 4) displays the expected negative deviations from linearity. In accordance with the presentation by Robin-

TABLE 3. Atomic fractional coordinates, isotropic temperature factors* (B in Å²), and occupancy factors** (G)

Atom	Parameter	X_{Mg}						
		0.00	0.30	0.36	0.51	0.69	0.75	1.00
M1	X	0.0	0.0	0.0	0.0	0.0	0.0	0.0
	Y	0.0	0.0	0.0	0.0	0.0	0.0	0.0
	Z	0.0	0.0	0.0	0.0	0.0	0.0	0.0
	B	0.22 (1)	0.49 (1)	0.32 (1)	0.34 (1)	0.34 (1)	0.33 (1)	0.40 (1)
(Mg)	G	0.5	0.232 (1)	0.188 (2)	0.108 (1)	0.051 (1)	0.033 (1)	0.0
	(Ni)	G	0.0	0.268 (1)	0.312 (2)	0.392 (1)	0.449 (1)	0.467 (1)
M2	X	0.9913 (2)	0.9903 (1)	0.9902 (1)	0.9906 (1)	0.9912 (1)	0.9916 (1)	0.9926 (1)
	Y	0.2773 (1)	0.2761 (1)	0.2758 (1)	0.2752 (1)	0.2744 (1)	0.2743 (1)	0.2738 (1)
	Z	0.25	0.25	0.25	0.25	0.25	0.25	0.25
	B	0.51 (1)	0.52 (1)	0.36 (1)	0.40 (1)	0.36 (1)	0.34 (1)	0.39 (1)
(Mg)	G	0.5	0.468 (1)	0.450 (2)	0.382 (1)	0.259 (1)	0.217 (1)	0.0
	(Ni)	G	0.0	0.032 (1)	0.050 (2)	0.118 (1)	0.241 (1)	0.283 (1)
Si	X	0.4261 (1)	0.4257 (1)	0.4257 (1)	0.4256 (1)	0.4263 (1)	0.4265 (1)	0.4273 (2)
	Y	0.0940 (1)	0.0937 (1)	0.0935 (1)	0.0936 (1)	0.0938 (1)	0.0938 (1)	0.0943 (1)
	Z	0.25	0.25	0.25	0.25	0.25	0.25	0.25
	B	0.37 (1)	0.42 (1)	0.27 (1)	0.30 (1)	0.30 (1)	0.29 (1)	0.33 (1)
O(1)	X	0.7658 (3)	0.7662 (3)	0.7667 (2)	0.7669 (3)	0.7675 (3)	0.7678 (3)	0.7689 (4)
	Y	0.0919 (1)	0.0926 (1)	0.0925 (1)	0.0932 (1)	0.0931 (1)	0.0934 (2)	0.0936 (2)
	Z	0.25	0.25	0.25	0.25	0.25	0.25	0.25
	B	0.50 (2)	0.53 (2)	0.40 (2)	0.40 (2)	0.38 (2)	0.38 (2)	0.45 (3)
O(2)	X	0.221 (3)	0.2193 (3)	0.2196 (2)	0.2188 (3)	0.2190 (3)	0.2182 (3)	0.2179 (4)
	Y	0.4470 (1)	0.4461 (1)	0.4459 (1)	0.4455 (1)	0.4452 (1)	0.4452 (1)	0.4451 (2)
	Z	0.25	0.25	0.25	0.25	0.25	0.25	0.25
	B	0.49 (2)	0.54 (2)	0.39 (2)	0.41 (2)	0.41 (2)	0.39 (2)	0.44 (3)
O(3)	X	0.2774 (2)	0.2761 (2)	0.2759 (2)	0.2756 (2)	0.2750 (2)	0.2748 (2)	0.2737 (3)
	Y	0.1630 (1)	0.1628 (1)	0.1627 (1)	0.1627 (1)	0.1627 (1)	0.1629 (1)	0.1629 (1)
	Z	0.0329 (2)	0.0321 (1)	0.0323 (1)	0.0317 (2)	0.0313 (2)	0.0311 (2)	0.0303 (2)
	B	0.52 (1)	0.56 (1)	0.42 (1)	0.45 (2)	0.44 (1)	0.41 (1)	0.51 (2)

* Isotropic equivalent of the anisotropic temperature factors (Hamilton, 1959).

** 0.5 represents full occupation.

TABLE 4. Anisotropic-temperature-factor coefficients ($\beta_{ij} \times 10^4$)

	ij	X_{Mg}						
		0.0	0.30	0.36	0.51	0.69	0.75	1.00
M1	11	173 (19)	501 (15)	252 (10)	257 (14)	269 (12)	232 (13)	306 (14)
	22	78 (4)	156 (3)	92 (2)	103 (3)	106 (3)	93 (3)	103 (4)
	33	127 (13)	314 (10)	250 (6)	263 (9)	249 (7)	278 (8)	359 (10)
	12	-7 (7)	-5 (3)	-1 (3)	-1 (2)	-3 (2)	-4 (3)	-11 (3)
	13	-47 (13)	-40 (5)	-33 (5)	-33 (4)	-31 (4)	-32 (5)	-42 (6)
	23	-35 (6)	-25 (3)	-23 (2)	-22 (2)	-25 (2)	-23 (2)	-22 (3)
M2	11	606 (25)	593 (24)	351 (18)	379 (19)	332 (15)	287 (16)	373 (14)
	22	119 (5)	118 (5)	77 (4)	90 (4)	85 (3)	69 (3)	76 (3)
	33	345 (15)	381 (16)	315 (12)	334 (12)	308 (9)	343 (10)	374 (10)
	12	-4 (9)	9 (6)	8 (5)	10 (4)	7 (4)	6 (4)	8 (3)
Si	11	337 (18)	414 (18)	178 (13)	189 (18)	220 (18)	160 (19)	174 (23)
	22	104 (4)	110 (4)	74 (3)	88 (3)	91 (4)	75 (4)	86 (5)
	33	269 (11)	305 (11)	247 (9)	267 (10)	240 (10)	290 (12)	356 (15)
	12	4 (6)	13 (5)	1 (4)	5 (5)	3 (6)	0 (6)	6 (8)
O(1)	11	397 (41)	473 (34)	253 (30)	268 (34)	301 (36)	212 (40)	269 (51)
	22	143 (9)	147 (8)	118 (7)	105 (8)	119 (8)	102 (9)	126 (12)
	33	390 (26)	386 (22)	350 (20)	370 (22)	288 (24)	386 (29)	423 (36)
	12	-8 (16)	19 (13)	21 (12)	-2 (13)	8 (14)	-2 (15)	32 (21)
O(2)	11	530 (43)	628 (35)	371 (31)	353 (35)	372 (38)	321 (43)	365 (51)
	22	101 (9)	110 (7)	84 (6)	82 (7)	97 (8)	72 (9)	87 (12)
	33	404 (27)	416 (23)	350 (20)	405 (23)	353 (25)	425 (30)	454 (38)
	12	12 (16)	5 (13)	-12 (12)	12 (13)	-13 (14)	-19 (15)	3 (20)
O(3)	11	508 (28)	629 (25)	371 (21)	409 (24)	386 (26)	379 (30)	393 (37)
	22	148 (6)	149 (5)	106 (5)	122 (5)	124 (6)	108 (6)	142 (9)
	33	343 (18)	354 (16)	335 (14)	340 (16)	323 (17)	319 (19)	436 (25)
	12	29 (11)	5 (9)	-8 (8)	16 (10)	5 (10)	14 (11)	19 (16)
	13	-0 (21)	-25 (16)	-30 (15)	-14 (17)	-19 (18)	15 (20)	-26 (26)
	23	53 (9)	49 (7)	47 (7)	46 (8)	41 (9)	17 (9)	54 (13)

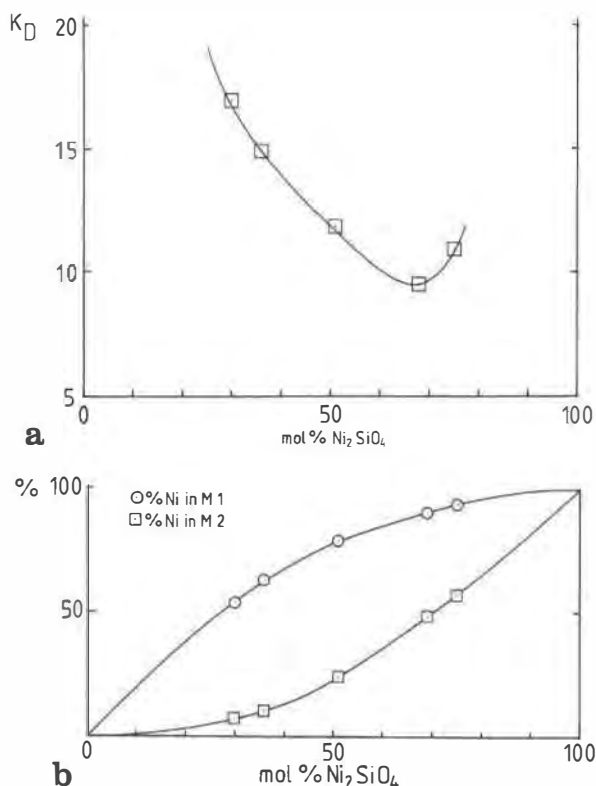


Fig. 1. Variation of (a) the intracrystalline distribution constant K_D (see text) and (b) the Ni content in M1 and M2 with composition.

son et al. (1971), these distortion parameters show a trend toward a more regular M1 octahedron.

M2 octahedron

As for M1, the mean M2–O distance is linearly related to $X_{Ni^{2+}}$ (Fig. 2). The lengths of the individual M2–O dis-

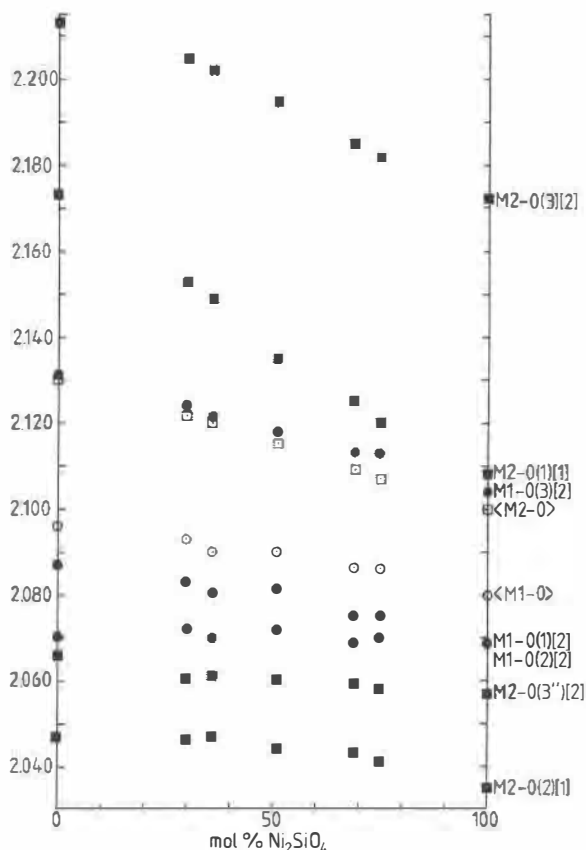


Fig. 2. Variation of octahedral metal–oxygen distances with composition. Figures in square brackets refer to the multiplicity of the bond.

tances are more scattered than those of the M1–O bonds, and they can be divided into two groups: (a) M2–O(1) and M2–O(3), which are directed toward the M1 octahedra, with the oxygens taking part in edge-sharing and

TABLE 5. Interatomic angles

	$X_{Ni^{2+}}$						
	0.00	0.30	0.36	0.51	0.69	0.75	1.00
Tetrahedron							
[1] O(1)–Si–O(2)	114.28 (8)	114.16 (7)	114.26 (6)	114.28 (7)	114.23 (7)	114.26 (8)	114.20 (11)
[2] O(1)–Si–O(3)	115.93 (5)	115.84 (4)	115.87 (4)	115.79 (4)	116.04 (5)	116.02 (5)	116.36 (6)
[2] O(2)–Si–O(3)	101.94 (5)	102.21 (4)	102.18 (4)	102.23 (4)	101.99 (5)	102.04 (5)	101.62 (7)
[1] O(3)–Si–O(3')	104.94 (8)	104.76 (7)	104.63 (6)	104.73 (7)	104.64 (7)	104.57 (8)	104.60 (10)
M1 octahedron							
[2] O(1)–M1–O(3)	58.06 (5)	84.83 (4)	84.79 (4)	84.67 (4)	84.69 (5)	84.59 (5)	84.56 (7)
[2] O(1)–M1–O(3')	94.94 (5)	95.17 (4)	95.21 (4)	95.33 (4)	95.31 (5)	95.41 (5)	95.44 (7)
[2] O(1)–M1–O(2)	86.68 (4)	87.06 (4)	87.06 (3)	87.22 (4)	87.24 (4)	87.29 (4)	87.29 (5)
[2] O(1)–M1–O(2')	93.32 (4)	92.94 (4)	92.94 (3)	92.78 (4)	92.76 (4)	92.71 (4)	92.71 (5)
[2] O(2)–M1–O(3')	105.05 (5)	104.69 (4)	104.67 (4)	104.53 (4)	104.39 (5)	104.40 (5)	104.32 (6)
[2] O(2)–M1–O(3)	74.95 (5)	75.31 (4)	75.33 (4)	75.47 (4)	75.61 (5)	75.60 (5)	75.68 (6)
M2 octahedron							
[2] O(1)–M2–O(3'')	90.78 (4)	91.11 (4)	91.22 (3)	91.20 (3)	91.20 (4)	91.12 (4)	90.96 (5)
[2] O(1)–M2–O(3)	81.10 (5)	81.25 (4)	81.26 (3)	81.52 (4)	81.75 (4)	81.82 (5)	81.97 (6)
[2] O(2)–M2–O(3)	96.74 (5)	96.74 (4)	96.69 (4)	96.75 (4)	96.68 (4)	96.79 (5)	96.88 (6)
[2] O(2)–M2–O(3'')	90.75 (4)	90.33 (4)	90.25 (3)	90.06 (3)	89.95 (4)	89.89 (4)	89.89 (5)
[1] O(3)–M2–O(3')	71.86 (6)	72.15 (5)	72.10 (4)	72.46 (5)	72.84 (5)	73.00 (6)	73.53 (7)
[2] O(3)–M2–O(3'')	88.73 (2)	88.95 (2)	89.05 (2)	89.09 (2)	89.18 (2)	89.17 (3)	89.25 (3)
[1] O(3'')–M2–O(3'')	109.94 (7)	109.29 (5)	109.18 (5)	108.76 (5)	108.25 (6)	108.10 (6)	107.39 (8)

Note: The number in square brackets refers to the multiplicity of the angle.

TABLE 6. Interatomic distances (Å)

	$X_{Ni^{2+}}$						
	0.00	0.30	0.36	0.51	0.69	0.75	1.00
Tetrahedron							
[1] Si-O(1)	1.615 (1)	1.616 (1)	1.618 (1)	1.617 (1)	1.615 (2)	1.616 (2)	1.617 (2)
[1] Si-O(2)	1.654 (2)	1.655 (1)	1.655 (1)	1.656 (1)	1.660 (2)	1.658 (2)	1.659 (2)
[2] Si-O(3)	1.637 (1)	1.639 (1)	1.639 (1)	1.639 (1)	1.639 (1)	1.641 (1)	1.643 (2)
(Si-O)	1.636	1.637	1.637	1.638	1.638	1.640	1.641
[1] O(1)-O(2)	2.746 (2)	2.746 (2)	2.749 (2)	2.749 (2)	2.751 (2)	2.749 (2)	2.750 (3)
[2] O(1)-O(3)	2.757 (2)	2.758 (1)	2.758 (1)	2.758 (1)	2.761 (2)	2.762 (2)	2.769 (2)
[2] O(2)-O(3)	2.557 (2)	2.564 (1)	2.562 (1)	2.564 (1)	2.564 (2)	2.564 (2)	2.559 (2)
[1] O(3)-O(3)	2.596 (2)	2.596 (2)	2.592 (2)	2.595 (2)	2.595 (2)	2.596 (2)	2.599 (3)
(O-O)	2.662	2.664	2.664	2.665	2.666	2.666	2.668
M1 octahedron							
[2] M1-O(1)	2.087 (1)	2.083 (1)	2.080 (1)	2.081 (2)	2.075 (1)	2.075 (1)	2.069 (1)
[2] M1-O(2)	2.070 (1)	2.072 (1)	2.070 (1)	2.072 (1)	2.069 (1)	2.070 (1)	2.068 (1)
[2] M1-O(3)	2.131 (1)	2.124 (1)	2.121 (1)	2.118 (1)	2.113 (1)	2.113 (1)	2.104 (1)
(M1-O)	2.096	2.093	2.090	2.090	2.086	2.086	2.080
[2] O(1)-O(3)	2.851 (2)	2.838 (1)	2.833 (1)	2.828 (1)	2.821 (2)	2.818 (2)	2.807 (2)
[2] O(1)-O(3')	3.108 (2)	3.106 (1)	3.103 (1)	3.104 (1)	3.096 (2)	3.097 (2)	3.087 (2)
[2] O(1)-O(2)	2.851 (2)	2.862 (2)	2.859 (2)	2.864 (2)	2.859 (2)	2.861 (2)	2.855 (3)
[2] O(1)-O(2')	3.023 (1)	3.013 (1)	3.009 (1)	3.007 (1)	3.000 (1)	2.999 (1)	2.993 (1)
[2] O(2)-O(3')	3.334 (2)	3.322 (1)	3.318 (1)	3.314 (1)	3.304 (2)	3.305 (2)	3.294 (2)
[2] O(2)-O(3)	2.557 (2)	2.564 (1)	2.562 (1)	2.564 (1)	2.564 (2)	2.564 (2)	2.559 (2)
(O-O)	2.954	2.951	2.947	2.947	2.941	2.941	2.933
M2 octahedron							
[1] M2-O(1)	2.173 (2)	2.153 (1)	2.149 (1)	2.135 (1)	2.125 (1)	2.120 (2)	2.108 (2)
[1] M2-O(2)	2.047 (2)	2.046 (1)	2.047 (1)	2.044 (1)	2.043 (1)	2.041 (2)	2.035 (2)
[2] M2-O(3)	2.213 (1)	2.205 (1)	2.202 (1)	2.195 (1)	2.185 (1)	2.182 (1)	2.172 (1)
[2] M2-O(3'')	2.066 (1)	2.060 (1)	2.061 (1)	2.060 (1)	2.059 (1)	2.058 (1)	2.057 (1)
(M2-O)	2.130	2.122	2.120	2.115	2.109	2.107	2.100
[2] O(1)-O(3'')	3.019 (2)	3.009 (1)	3.009 (1)	2.998 (1)	2.990 (2)	2.984 (2)	2.970 (2)
[2] O(1)-O(3)	2.851 (2)	2.838 (1)	2.833 (1)	2.828 (1)	2.821 (2)	2.818 (2)	2.807 (2)
[2] O(2)-O(3)	3.186 (2)	3.179 (1)	3.176 (1)	3.171 (1)	3.160 (2)	3.159 (2)	3.149 (2)
[2] O(2)-O(3''')	2.927 (2)	2.912 (1)	2.911 (1)	2.903 (1)	2.899 (2)	2.896 (2)	2.891 (2)
[1] O(3)-O(3')	2.596 (2)	2.596 (2)	2.592 (2)	2.595 (2)	2.595 (2)	2.596 (2)	2.599 (3)
[2] O(3)-O(3')	2.993 (1)	2.990 (1)	2.991 (1)	2.987 (1)	2.981 (1)	2.978 (2)	2.972 (2)
[1] O(3'')-O(3''')	3.383 (2)	3.360 (2)	3.359 (2)	3.349 (2)	3.338 (2)	3.333 (2)	3.316 (3)
(O-O)	2.994	2.984	2.983	2.977	2.970	2.967	2.958

Note: The number in square brackets refers to the multiplicity of the bond.

(b) M2-O(3'') and M2-O(2) pointing out from the chains. The former undergo considerable decreases, whereas the latter show barely significant changes. The bond M2-O(2) has a significant positive deviation from linearity (Fig. 2). It is therefore apparent that the main shrinkage of the M2 octahedra can be attributed to the decrease of the M2-O bonds directed toward the center of the chains.

The variation in the volume of the M2 octahedron with composition is linear (Fig. 3), and the distortion parameter, OAV, has a small positive deviation (Fig. 4).

Si tetrahedron

Brown (1980) reported a grand mean Si-O distance of 1.636 ± 0.004 Å from a compilation of 45 olivines. The mean Si-O distances obtained in the present work vary from 1.636 Å for pure Mg₂SiO₄ to 1.641 Å for pure Ni₂SiO₄ (Table 6), in good agreement with the above value. The distortion parameter tetrahedral-angle variance (TAV) (Table 7) indicates that the Si tetrahedron is more distorted in Ni₂SiO₄ than in Mg₂SiO₄.

TABLE 7. Polyhedral distortion parameters* and octahedral volumes (V_{M1} and V_{M2})

	$X_{Ni^{2+}}$						
	0.00	0.30	0.36	0.51	0.69	0.75	1.00
V_{M1} (Å ³)	11.800 (7)	11.770 (7)	11.733 (6)	11.727 (7)	11.657 (7)	11.662 (8)	11.569 (9)
V_{M2} (Å ³)	12.408 (8)	12.288 (7)	12.268 (7)	12.191 (8)	12.124 (8)	12.084 (9)	11.985 (11)
TAV	48.1 (2)	46.1 (2)	46.9 (2)	46.0 (2)	48.8 (2)	48.6 (3)	52.8 (3)
OAV _{M1}	95.2 (2)	91.3 (2)	91.2 (2)	89.9 (2)	88.3 (2)	88.7 (2)	88.0 (2)
OAV _{M2}	89.2 (2)	85.4 (2)	85.0 (2)	81.7 (2)	77.9 (2)	76.9 (2)	72.7 (3)

* TAV (tetrahedral-angle variance) = $\sum_{i=1}^6 (A_i - 109.47)^2/5$, where A_i values are the tetrahedral angles O-T-O. OAV (octahedral-angle variance) =

$\sum_{i=1}^{12} (A_i - 90)^2/11$, where A_i values are the angles O-M-O.

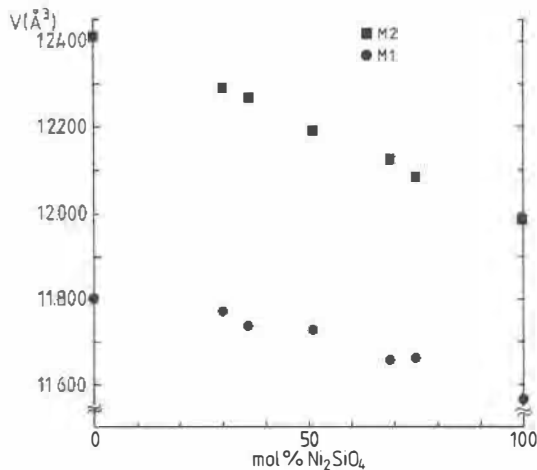


Fig. 3. Volumes of the occupied octahedra vs. composition.

Cell parameters

The relative shrinkages of the cell parameters from Mg_2SiO_4 to Ni_2SiO_4 are 0.53%, 0.76%, and 1.07% for a , b and c , respectively. Since the c axis is parallel to the edge-sharing M1–M1–M1 spine of the zigzag octahedral chain, a change in the M1 octahedron size has a significant influence on the c axis. The shrinkage of a is smaller because every second octahedral chain in this direction is unoccupied.

The reason for the peculiar shape of the b dimension curve (Fig. 5) in the Mg-rich compositions is somewhat unclear. This same feature has earlier been recognized by Matsui and Syono (1968). In the M1 octahedron, there is a slight increase in the O(2)–O(3) distance in the b direction (Table 6). This is surprising considering the great increase of Ni^{2+} in the M1 octahedron (see Fig. 5b). The expansion of the M1 octahedron in this direction together with a minor shrinkage of the M2 octahedron [see O(2)–O(3) in M2, Table 6] can explain the special shape of the b -axis curve.

In an attempt to understand the relationship between the lattice parameters and the mean ionic radii of the cations, Lumpkin and Ribbe (1983) used 52 known olivine structures. They concluded that the a dimension is

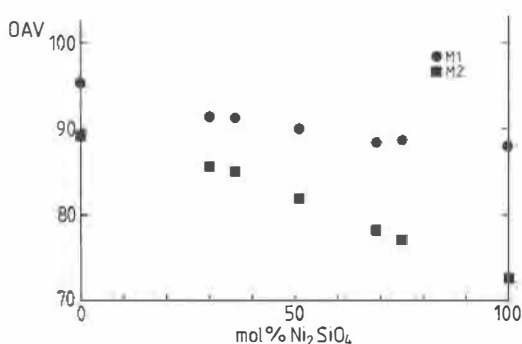


Fig. 4. Variation of the octahedral distortion parameter, OAV, with composition (see Table 7 for definitions).

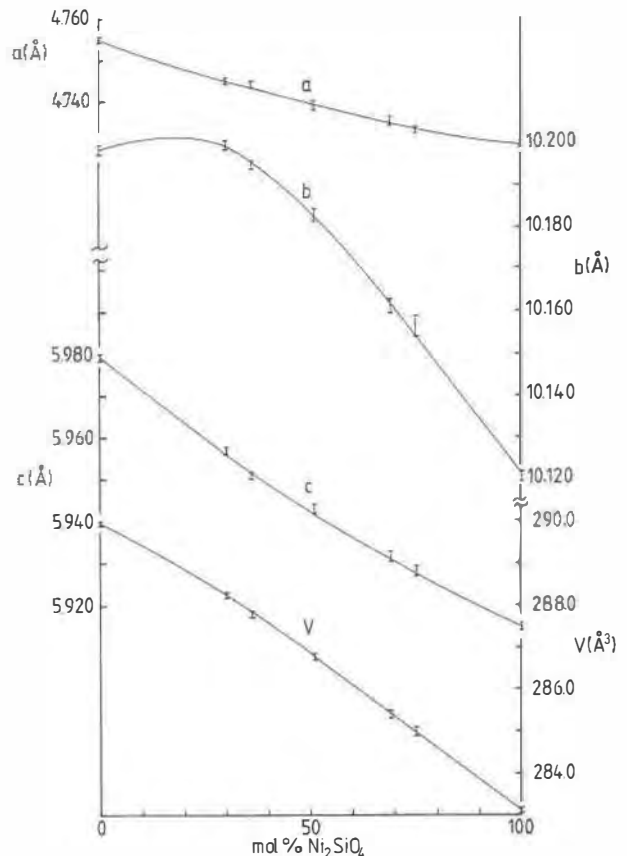


Fig. 5. Variation in the unit-cell parameters of the Ni-Mg olivine solid solution. The vertical bars represent $2 \times \text{S.D.}$

highly correlated to r_{M1} and the b dimension to r_{M2} , whereas the c dimension is dependent on both r_{M1} and r_{M2} . The mean cation radii r_{M1} and r_{M2} were calculated using the cation occupancies of M1 and M2 and the ionic radii for Mg^{2+} and Ni^{2+} as given by Shannon (1976). It was emphasized by Lumpkin and Ribbe (1983) that their equations and the a vs. b plot are more successful in cases where $|r_{\text{M1}} - r_{\text{M2}}| > 0.1 \text{ \AA}$. Although the difference in ionic radius for Ni^{2+} and Mg^{2+} is only 0.03 \AA , it was nevertheless of interest to apply their equations for silicate olivines (see Table 8) in constructing an a vs. b plot for the present system (see Fig. 6). Data from this study, together with data from Bish (1981) and Rajamani et al. (1975), are shown in this diagram. Both experimental and corresponding calculated (from the equations) a - b values are plotted for each sample. The two points, which in the ideal case should coincide, show at least a rough correspondence. This implies that the qualitative predictions of the diagram are correct.

The situation for the liebenbergite (Bish, 1981) is complicated by its content of Fe^{2+} and Co^{2+} (4.5% and 2.5%, respectively). Consequently the composition predicted by the diagram becomes richer in Mg^{2+} than that given by the analysis.

It must be pointed out that the estimated uncertainties

TABLE 8. Cell-dimension equations

Cell dimension	Equations					
	Lumpkin and Ribbe (1983)					
a (Å)	=	$0.932r_{M1}$	+	$0.236r_{M2}$	+	3.918
0.010		0.036		0.020		0.025
b (Å)	=	$0.505r_{M1}$	+	$3.211r_{M2}$	+	7.535
0.025		0.089		0.046		0.061
c (Å)	=	$1.231r_{M1}$	+	$1.484r_{M2}$	+	4.010
0.019		0.068		0.035		0.047
V (Å ³)	=	$149.4r_{M1}$	+	$187.6r_{M2}$	+	46.8
1.643		5.7		3.0		4.0
	Present study					
a (Å)	=	$0.5976r_{M1}$	+	$0.2443r_{M2}$	+	4.1487
0.0005		0.032		0.031		0.015
b (Å)	=	$-0.1708r_{M1}$	+	$2.7738r_{M2}$	+	8.3247
0.0013		0.079		0.076		0.036
c (Å)	=	$1.311r_{M1}$	+	$0.7787r_{M2}$	+	4.474
0.0012		0.073		0.070		0.033
V (Å ³)	=	$95.6r_{M1}$	+	$129.6r_{M2}$	+	127.8
0.04		2.7		2.6		1.2

Note: The figures below the cell parameters and coefficients in the equations represent their standard deviations.

(taken as $2 \times$ S.D.) in the regression equations, ± 0.02 Å and ± 0.05 Å, are of the same order of magnitude as the total changes in a and b . The latter are 0.035 Å and 0.11 Å, respectively. A set of equations analogous to those of Lumpkin and Ribbe, for the Ni-Mg binary alone, was also determined from cell parameters and refined M1 and M2 site occupancies obtained in the present study. Not unexpectedly, the agreement is better in this case (see Table 8). In the a - b plot based on these new equations (Fig. 6b), the total spread of the a and b is smaller: about 0.002 Å and 0.005 Å, respectively. It should also be observed that the b dimension for ordered Mg^{2+} -rich compositions is longer than for Mg_2SiO_4 . This behavior resembles the situation found in the a - b plot for the Fe-Mn olivines as discussed by Annersten et al. (1984) and by Miller and Ribbe (1985).

The Figure 6b plot provokes some further comment. The two synthetic olivines of Bish (1981) and Rajamani et al. (1975) show significant discrepancies between experimental and calculated values of a and b . The complications associated with the liebenbergite persist, of course, in Figure 6b. Here the a and b dimensions lie outside the triangular plot, below the line of complete ordering. If Co^{2+} and Fe^{2+} are considered to be completely ordered on M2, the corrected calculated a - b values lie on the line of complete ordering.

As pointed out by Miller and Ribbe (1985), the success of this determinative method is dependent on good chemical analysis, accurate cell dimensions, and unambiguous site occupancies. In the Ni-Mg binary, where the cell-dimension differences are small, the importance of accurate cell-parameter determination should be stressed. The plot presented in this study (Fig. 6b), based on the seven olivines investigated within the Ni-Mg binary, is clearly more suitable for predicting ordering and com-

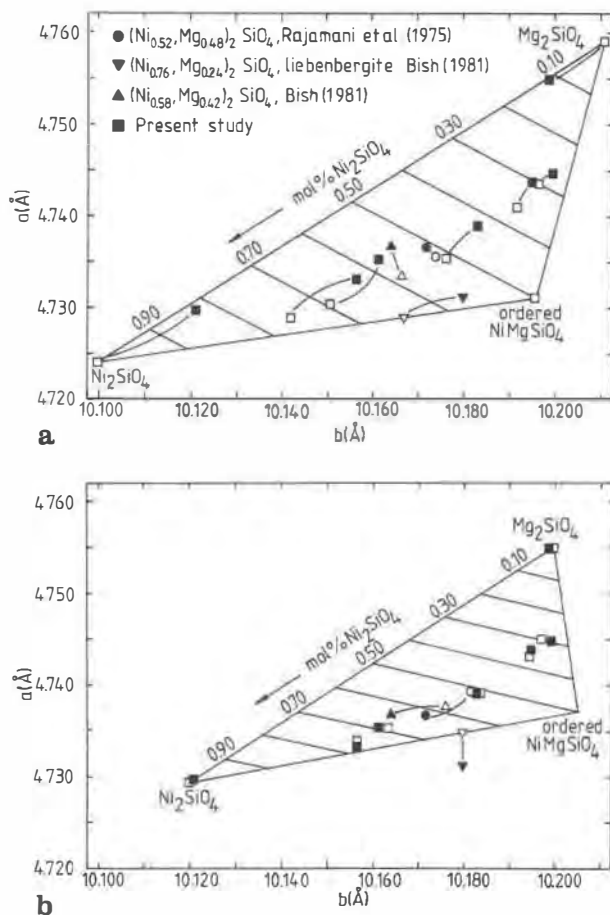


Fig. 6. Triangular plots of a against b as calculated from the equations in Table 8. (a) Based on the silicate olivine equations of Lumpkin and Ribbe (1983). (b) Based on the equations from the present study. Open symbols represent calculated values, using refined occupancies and the equations in Table 8. The filled symbols show the corresponding experimental values.

position in this system than the Figure 6a plot based on the general silicate regression equations.

CONCLUSIONS

Cation ordering in the five Ni-Mg olivines investigated shows a considerable compositional dependence. The ordering increases toward the end members, especially toward pure Mg_2SiO_4 . The general trend of octahedral properties (volume, mean and individual distances) shows a nearly linear relationship to $X_{Ni^{2+}}$. This is a somewhat unexpected observation. It is natural to expect these properties to respond more directly to the cation content of the octahedra, and thus be linearly related to the specific octahedral composition. The distortion parameter OAV of M1 and that of M2 seem to be the only calculated properties of the octahedra that agree with the expected trends.

Equations relating lattice parameters to site occupancies are based upon the mean radii r_{M1} and r_{M2} , but these

are not linearly related to $X_{Ni^{2+}}$ since they are calculated from the refined site occupancies and the ionic radii of Shannon (1976). No evidence of a direct structural correspondence with these mean octahedral-cation radii has been found in this system, and it may therefore seem contradictory to use these mean radii to determine order and composition. On the other hand, the coefficients of r_{M1} and r_{M2} in the equations reflect the nonuniform influence of the cation contents of M1 and M2 on the cell dimensions. This influence involves not only geometrical changes in the octahedron, but also in all other occupied and empty sites along the cell edge. These anisotropic effects are not necessarily displayed in quantities such as octahedral volume and mean M-O distances. So, even if the concept of mean octahedral-cation radius is not relevant in its strictest sense, the idea of relating cell-dimension changes to octahedral-site content may be valid.

ACKNOWLEDGMENTS

The author wishes to thank Professors Erik Rosén and John O. Thomas for valuable discussions and helpful suggestions. Dr. Britt Hedman is also acknowledged for many constructive comments. Thanks are also due to Professor Alberto dal Negro for the microprobe analysis in Padova, Italy. Financial support from the Swedish Natural Science Research Council is gratefully acknowledged.

REFERENCES

- Annersten, H., Adetunji, J., and Filipides, A. (1984) Cation ordering in Fe-Mn silicate olivines. *American Mineralogist*, 69, 1110-1115.
- Bish, D.L. (1981) Cation ordering in synthetic and natural Ni-Mg olivine. *American Mineralogist*, 66, 770-776.
- Brown, G.E., Jr. (1980) Olivines and silicate spinels. *Mineralogical Society of America Reviews in Mineralogy*, 5, 276-279.
- Cruikshank, D.W.J. (1965) Errors in least-squares methods. In J.S. Rollet, Ed., *Computing methods in Crystallography*. Pergamon Press, New York.
- Hamilton, W.C. (1959) On the isotropic temperature factor equivalent to a given anisotropic temperature factor. *Acta Crystallographica*, 12, 609-610.
- International tables for X-ray crystallography (1974). Volume IV. Kynoch Press, Birmingham, England. (Present distributor D. Reidel, Dordrecht.)
- Lehmann, M.S., and Larsen, F.K. (1974) A method for location of the peaks in step-scan-measured Bragg reflexions. *Acta Crystallographica*, A30, 580-584.
- Lumpkin, G.R., and Ribbe, P.H. (1983) Composition, order-disorder and lattice parameters of olivines: Relationships in silicate, germanate, beryllate, phosphate and borate olivines. *American Mineralogist*, 68, 164-176.
- Lundgren, J.-O. (1982) Crystallographic computer programs. Report UUIC-B13-4-05. Institute of Chemistry, University of Uppsala.
- Matsui, Y., and Syono, Y. (1968) Unit cell dimensions of some synthetic olivine group solid solutions. *Geochemical Journal*, 2, 51-59.
- Miller, M.L., and Ribbe, P.H. (1985) Methods for determination of composition and intracrystalline cation distribution in Fe-Mn and Fe-Ni silicate olivines. *American Mineralogist*, 70, 723-728.
- Princivalle, F., and Secco, L. (1985) Crystal structure refinement of 13 olivines in the forsterite-fayalite series from volcanic rocks and ultramafic nodules. *Tschermaks Mineralogische und Petrologische Mitteilungen*, 34, 105-115.
- Rajamani, V., Brown, G.E., and Prewitt, C.T. (1975) Cation ordering in Ni-Mg olivine. *American Mineralogist*, 60, 292-299.
- Robinson, K., Gibbs, G.V., and Ribbe, P.H. (1971) Quadratic elongation: A quantitative measure of distortion in coordination polyhedra. *Science*, 172, 567-570.
- Shannon, R.D. (1976) Revised effective ionic radii and systematic studies of interatomic distances in halides and chalcogenides. *Acta Crystallographica*, A32, 343-352.

MANUSCRIPT RECEIVED JULY 22, 1986

MANUSCRIPT ACCEPTED MAY 21, 1987